# TAU-106K: A NEW DATASET FOR COMPREHENSIVE UNDERSTANDING OF TRAFFIC ACCIDENT

**Yixuan Zhou**[1,2,*] **Long Bai**[1,3,*] **Sijia Cai**[1,†,‡] **Bing Deng**[1] **Xing Xu**[2,4,‡] **Heng Tao Shen**[2,4]

[1] Alibaba Cloud [2] University of Electronic Science and Technology of China (UESTC)
[3] The Chinese University of Hong Kong (CUHK) [4] Tongji University (Tongji)

{yixuanzhou.zyx, bailong.bai, stephen.csj, dengbing.db}@alibaba-inc.com,
xing.xu@uestc.edu.cn, shenhengtao@hotmail.com

## ABSTRACT

Multimodal Large Language Models (MLLMs) have demonstrated impressive performance in general visual understanding tasks. However, their potential for high-level, fine-grained comprehension, such as anomaly understanding, remains unexplored. Focusing on traffic accident, a critical and practical scenario within anomaly understanding, we investigate the advanced capabilities of MLLMs and propose TABot, a multimodal MLLM specialized for accident-related tasks. To facilitate this, we first construct TAU-106K, a large-scale multimodal dataset containing 106K traffic accident videos and images collected from academic benchmarks and public platforms. The dataset is meticulously annotated through a video-to-image annotation pipeline to ensure comprehensive and high-quality labels. Building upon TAU-106K, we train TABot using a two-step approach designed to integrate multi-granularity tasks, including accident recognition, spatial-temporal grounding, and an auxiliary description task to enhance the model's understanding of accident elements. Extensive experiments demonstrate TABot's superior performance in traffic accident understanding, highlighting not only its capabilities in high-level anomaly comprehension but also the robustness of the TAU-106K benchmark. Our code and data will be available at https://github.com/cool-xuan/TABot.

## 1 INTRODUCTION

Traffic Accident Detection (TAD) has always been a crucial and practical task in public safety and transportation management. The development of advanced technologies, such as computer vision and deep learning, has enabled the automation of TAD, providing real-time accident alerts and analysis. Despite significant research on traffic accident detection (Shah et al., 2018; Zhu et al., 2019; Kim et al., 2019; Haresh et al., 2020; Ghahremannezhad et al., 2022), existing TAD methods often rely on conventional visual feature extraction techniques that lack high-level comprehension and multimodal alignment capabilities in interpreting intricate spatial-temporal dynamics.

Recent advancements in aligning large language models (LLMs) on visual-language datasets have driven remarkable progress in multi-modal understanding tasks (Achiam et al., 2023). With extensive pre-training and instruction tuning, multimodal LLMs (MLLMs) have demonstrated superior performance in spatially visual understanding and logical reasoning for the general-purpose comprehension (Li et al., 2023; Zhu et al., 2023; Liu et al., 2024). However, due to the inherent gap between general and specific tasks, MLLMs trained on general domains often underperform in specialized fields due to limited domain-specific data. For instance, as illustrated in Figure 1, the most advanced MLLMs, such as GPT-4o (Achiam et al., 2023), Qwen2-VL (Yang et al., 2024), and

[*] Work done during an internship at Alibaba Cloud.
[†] Project lead.
[‡] Corresponding authors.

**Question:** Do you notice any traffic accident scenarios in this picture? Please respond with a 'Yes' or 'No'. Following that, describe the image in one sentence.

**GPT-4o:** No, the image shows a busy city intersection with vehicles and motorcycles waiting at a traffic light.
**Qwen2-VL:** No. The image shows a busy urban street with cars, scooters, and pedestrians, but there is no visible accident.
**Gemini-1.5-Pro:** No. The image shows a sunny city street scene with several motorbikes and cars at an intersection under a highway overpass.
**TABot-Chat (Ours):** Yes. Because a black car brake was not on time, it collided with a white coat electric bicycle rider.

Figure 1: One example to illustrate the limitations of general MLLM in understanding traffic accidents. In the scenario where a vehicle collision occurs due to a sudden lane change by the leading vehicle, **GPT-4o**, **Qwen2-VL**, and **Gemini-1.5-Pro** *fail* to detect this issue.

Gemini-1.5-Pro (Team et al., 2024), may misinterpret the visual content of traffic accidents where a vehicle collision occurs, leading to inaccurate responses. We argue that the failure of general MLLMs to understand traffic accidents stems from the following two main reasons: (i) Traffic accident detection requires MLLMs to grasp ambiguous concepts like *anomaly* and *accident*, which are context-dependent and defined by human criteria. However, existing MLLMs are trained on general-purpose data focusing on fundamental semantics, lacking the specialized understanding of such high-level semantics. (ii) The visual representations of accident occurrences differ significantly from general scenes, necessitating realigning these visual representations with the semantic understanding towards traffic accidents. Both of these limitations highlight the need for infrastructure that includes accident-specific annotations and specialized MLLMs to understand traffic accidents.

To pioneer an MLLM specialized in traffic accident comprehension, we first created **TAU-106K**, a large-scale multimodal traffic accident dataset containing 106K videos and images with detailed accident-oriented annotations. In particular, we aggregate academic benchmarks and crawl traffic accident videos from public platforms, building a diverse and high-quality visual foundation. To ensure annotation quality and efficiency, we design a video-to-image annotation pipeline, resulting in comprehensive annotations that are manually crafted by human labors. The annotations cover accident recognition, description, temporal localization, and spatial grounding at both the image and video levels, providing detailed and structured information for MLLMs to understand traffic accidents.

Using TAU-106K, we reorganize the annotations into instructional data to unlock MLLMs' potential in traffic accident understanding and introduce **TABot**, an end-to-end MLLM specialized for traffic accident comprehension across both image and video modalities. We adopt a two-step training approach: functional tuning to engage multi-granularity accident detection capabilities activation, and instruction tuning to enhance contextual comprehension and instruction following capabilities. In particular, during functional tuning, we propose two training strategies to serve temporal localization, the most crucial task in traffic accident understanding: (i) Negative Segment Referring (NSR), which utilizes contrastive learning to heighten the model's sensitivity to accident boundaries, and (ii) Video Spatial Alignment (VSA), which inserts spatial information into the training of video tasks, serving as a fine-grained complement to temporal localization. Followed by the functional tuning, we further generate multi-turn dialogues using an automated paradigm (Liu et al., 2024) and perform instruction tuning to enhance the dataset's utility and capabilities of MLLMs for human-like chatting and traffic accident understanding.

## 2 Related Work

**Multimodal Large Language Models.** Extensive research has focused on enabling LLMs to process visual information, typically by adding an adapter between pre-trained visual models and LLMs to align features from different modalities (Li et al., 2023; Zhu et al., 2023; Liu et al., 2024). Some advanced multimodal LLMs, such as Qwen2-VL (Yang et al., 2024), unified image and video un-

derstanding into a single model, but still struggle with more fine-grained tasks. On the side of image modal, object grounding has been a key focus, with a series of works (Chen et al., 2023b; Bai et al., 2023; Peng et al., 2023; Chen et al., 2023c; You et al., 2023) standardizing grounding coordinates to text format and achieving robust grounding capabilities. On the other hand, videos, as a more complex form of visual data, introduce greater challenges in aligning with video content (Maaz et al., 2023; Lin et al., 2023; Chen et al., 2023a; Zhang et al., 2023; Qian et al., 2024; He et al., 2024; Cheng et al., 2024; Xu et al., 2024; Zhang et al., 2024; Chen et al., 2023d; 2024). VTimeLLM (Huang et al., 2024) and TimeChat (Ren et al., 2024) address temporal localization by proposing time-aware attention mechanisms. GroundingGPT (Li et al., 2024) unified fine-grained capabilities across image and video for comprehensive multimodal understanding. Despite these advancements, previous works focus on general-purpose understanding, remaining largely unexplored in some specific scenarios, such as traffic accident understanding.

**Traffic Accident Detection and Understanding.** Traditional Traffic Accident Detection (TAD) methods are classified into single-stage (Hasan et al., 2016) and two-stage paradigms (Yao et al., 2019; Fang et al., 2022b). Single-stage approaches often rely on frame-to-frame errors but underperform in forecasting non-ego accidents and are sensitive to dynamic backgrounds (Hasan et al., 2016). Two-stage methods extract visual features, such as bounding boxes and optical flow, and apply TAD models to predict anomalies (Fang et al., 2022b). However, these methods depend heavily on the quality of feature extraction. Recent advances have integrated textual information into TAD, with TTHF (Liang et al., 2024) introducing text-driven attention mechanisms for anomaly detection in videos, and SUTD-TrafficQA (Xu et al., 2021) modeling fundamental question-answering and reasoning tasks for traffic accident scenes. On the MLLM front, empirical studies (Cao et al., 2023) have validated GPT-4(V)'s effective recall and description capabilities for traffic accident images. To this end, the potential of MLLMs in accident understanding remains unexplored, particularly in spatial-temporal grounding and reasoning over traffic accident videos.

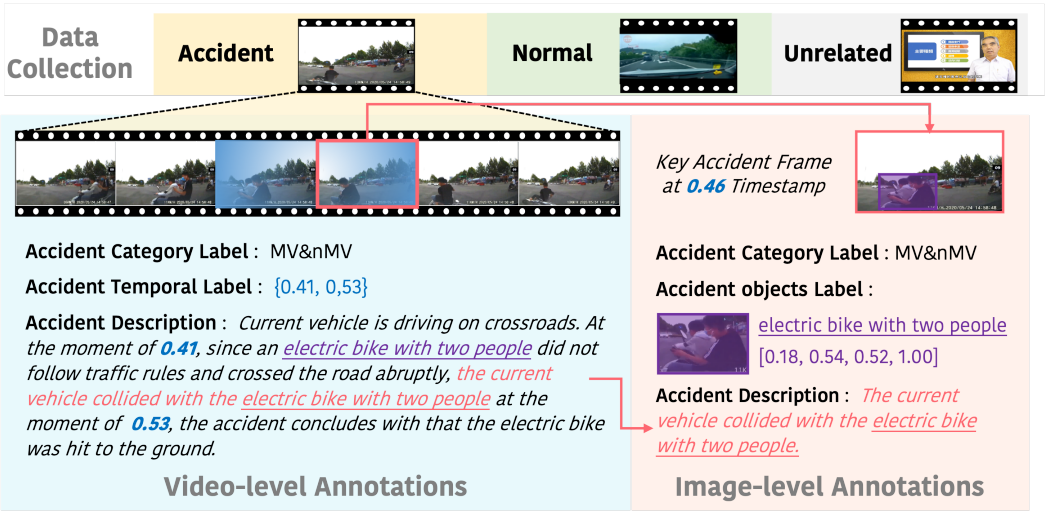


Figure 2: The data collection and annotation pipeline for building TAU-106K.

## 3 TAU-106K FOR VIDEO-IMAGE TRAFFIC ACCIDENT UNDERSTANDING

To advance the development of MLLMs for traffic accident analysis, we introduce TAU-106K, a comprehensive dataset integrating video and image data for traffic accident understanding, manually labeled with multi-granularity annotations through a video-to-image annotation pipeline (Figure 2).

### 3.1 VIDEO-BASED DATA COLLECTION AND ANNOTATION

**Video Data Collection and Preprocessing.** While traffic accident understanding is a critical public safety task and has been extensively studied, the available open-source benchmarks are limited in both scale and diversity, often featuring low-resolution video data. To address this, we aggregate

established traffic accident benchmarks such as TAD (Xu et al., 2022), DoTA (Yao et al., 2022), and CCD (Bao et al., 2020), selecting high-quality video clips as the data foundation for further annotation. We further expand the dataset by crawling road surveillance and dashcam footage from platforms like *YouTube* and *BiliBili*, capturing diverse real-world traffic conditions. Despite the abundance of traffic accident videos on the Internet, they are often unstructured and lack annotations. For the crawled raw videos, we first crop them into individual clips using the scene change detection toolkit `PySceneDetect`, and then manually filter out irrelevant or low-quality videos. Consequently, we obtain a collection of 51.5K traffic-focused video clips sourced from academic benchmarks and social media platforms, as illustrated in the upper part of Figure 2.

**Video-based Accident Annotations.** All existing benchmarks for traffic accident understanding lack comprehensive annotations, especially in terms of accident descriptions, which are crucial for enabling MLLMs to understand accident events in detail. To bridge this gap, we annotate from scratch or supplement existing annotations in three key aspects:

1. Accident Category: accident occurrence and detailed accident types. Each clip is reviewed to determine if an accident is present, labeled either as *Accident* or *Normal*. For *Accident* clips, we further categorize the accident type into five subcategories: single motor vehicle (SMV) accident, multiple motor vehicle (MMV) accident, multiple non-motor vehicle (MnMV) accident, motor vehicle and non-motor vehicle (MV&nMV) accident, and vehicle and pedestrian (V&P) accident.

2. Accident Duration: the specific time points of the accident occurrence. Annotators precisely identify the start and end timestamps of the accident within each clip, yielding the time points $\{t_{start}, t_{end}\}$. In particular, the start time $t_{start}$ should be the exact frame when the accident event begins, such as the moment of collision, while the end time $t_{end}$ is marked when the event concludes (e.g., stopping). Both timestamps are normalized within the clip duration to ensure consistency.

3. Accident Description: a detailed textual description of the nature of the accident, which is absent in all existing traffic accident benchmarks while being substantial for MLLMs to understand the accident event in detail. To ensure consistency and precision, we design a structured annotation template, guiding annotators to provide detailed and structured descriptions of the accident events.

The description template for *Accident* is structured to depict the **Traffic Scenario** (urban, highway, etc.), **Accident Content** including the objects involved in the accident (vehicles, pedestrians, etc.) and the nature of the accident (collision, scrape, etc.), and **Aftermath**, ensuring comprehensive and structured annotations. The labeled start and end timestamps are also incorporated into the description to provide temporal context for the accident event. Beyond the accident event itself, annotators are also encouraged to infer the **Potential Causes**, such as traffic rule violations or improper driving behaviors. The detailed template is also dependent on the **Footage Source**, either *Dashcam* or *Surveillance camera*. For intuitive understanding, we decompose the example shown in Figure 2 into the structured format in the gray block.

> [**Footage Source:** Current vehicle is driving on] [**Traffic Scenario:** crossroads]. At the moment of 0.41, [**Potential Causes:** since an electric bike with two people did not follow traffic rules and crossed the road abruptly], [**Accident Content:** the current vehicle collided with the electric bike with two people], at the moment of 0.53, [**Aftermath:** the accident concludes with that the electric bike was hit to the ground.]

In practice, these three annotation tasks are performed simultaneously, with multiple rounds of review and correction to ensure quality and consistency. This integrated approach ensures coherence in annotations, reflecting the interconnected nature of these tasks.

### 3.2 Image-based Data Collection and Annotation

The above video annotations are multi-granularity while lacking spatial details, which are crucial for MLLMs to understand fine-grained visual features. To address this, we further derive images from the video clips and label them with detailed spatial information, whose detailed annotation pipeline is illustrated in the bottom right part of Figure 2.

**Image Data Collection and Selection.** Besides a few image-only accident datasets (e.g., Task-Fix (Juan et al., 2021)), most of the image data in our TAU-106K is sampled from the video clips.

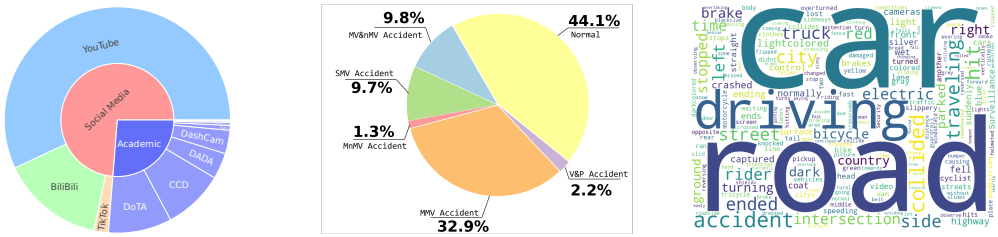


(a) Data source distribution. (b) Accident type distribution. (c) Word cloud of description.

Figure 3: Data source distribution, accident type distribution, and word cloud of accident descriptions in TAU-106K dataset.

Guided by the temporal localization annotations in the video clips, we first extract candidate frames by uniformly sampling frames within the labeled accident duration. These frames are then evaluated by annotators to select keyframes that best represent the accident events, based on the *Accident Description* in the video annotations. Notably, the time points of the selected keyframes are preserved to keep the temporal connection between the video and image data, which also enables our video spatial alignment strategy in model training. In addition to accident-related frames, we randomly sample accident-free frames to maintain data balance and prevent model bias.

**Image Annotations Derived from Video Annotations.** For the images sourced from existing benchmarks, we adopt the available annotations and extend them to our multi-granularity annotations. On the other hand, for the images derived from video data, we inherit the accident-related annotations from the video clips, including the *Accident Category* and *Accident Description*, where the latter extracted from the *content of the accident* part in the video-based accident description to maintain annotation consistency and reduce workload. In particular, labels for the involved objects are derived directly from the accident descriptions, ensuring that the annotated objects are those explicitly mentioned. For instance, given the accident description as "*A blue car collides with a pedestrian in white clothes*", the corresponding objects will be labeled as *blue car* and *pedestrian in white clothes*, respectively. This instance-specific labeling helps MLLMs focus on the objects directly involved in the accident, minimizing distractions from irrelevant objects of the same category that may appear in the scene.

Table 1: The comparison of TAU-106K with other accident-specific or general-purpose benchmarks. CLS': Accident Categories, 'TL': Temporal Annotation, 'Bbox': Object Grounding Annotation, 'CAP': Caption Annotation, and 'QA': Question-Answer Pairs.

| Dataset | Years | Domain | # Videos | Annotations | Avg. Words | Avg. Duration |
|---|---|---|---|---|---|---|
| Dashcam (Chan et al., 2017) | 2016 | Traffic | 3,000 | TL; | - | 5.0 seconds |
| A3D (Yao et al., 2019) | 2019 | Traffic | 1,500 | TL; | - | 8.5 seconds |
| CCD (Bao et al., 2020) | 2021 | Traffic | 1,500 | TL; | - | 5.0 seconds |
| TAD (Lv et al., 2021) | 2021 | Traffic | 500 | CAP; TL; | - | 35.8 seconds |
| DADA (Fang et al., 2021) | 2021 | Traffic | 200 | CAP; TL; Driver Attention | - | 11.0 seconds |
| SUTD-TrafficQA (Xu et al., 2021) | 2021 | Traffic | 10,080 | QA pairs | - | 13.6 seconds |
| DoTA (Yao et al., 2022) | 2022 | Traffic | 4,677 | CAP; TL; Bbox | - | 15.6 seconds |
| CAP (Fang et al., 2022a) | 2023 | Traffic | 11,727 | CAP; TL; Fixed-Form CAP | 6.3 | 6.2 seconds |
| **TAD-106K (Ours)** | 2024 | Traffic | 51,544 | CAP; TL; Bbox; Free-Form CAP | 32.1 | 10.3 seconds |
| Charades-STA (Gao et al., 2017) | 2017 | Daily | 9,848 | TL; Free-Form CAP | 6.3 | 31 seconds |
| DiDeMo (Anne Hendricks et al., 2017) | 2017 | Open | 10,464 | TL; Free-Form CAP | 7.5 | 30 seconds |
| ActivityNet-Captions (Krishna et al., 2017) | 2017 | Open | 19,209 | TL; Free-Form CAP | 13.5 | 180 seconds |

### 3.3 Data Statistics and Analysis

TAU-106K comprises 106K multimodal data instances, including 51.5K video clips and 54.8K images, all with high-quality annotations. The majority of the video clips and images are in 720p resolution and are sourced from both open-source benchmarks and social media platforms, as shown in Figure 3(a). Among the TAU-106K, 56% of instances are labeled as *Accident* and 44% as *Normal*, with detailed category distribution shown in Figure 3(b). The balanced distribution of accident-related and accident-free instances ensures that the model is trained robustly, avoiding biases towards accident occurrences. The average video duration of processed and filtered clips is 10.3 seconds, with annotated accidents lasting an average of 3 seconds (approximately 25% of the video clip). As for the image data, 45K accident-involved objects are grounded, with an average of 1.6 bounding boxes per image and an average bounding box area covering 7.9% of the image. Our accident de-

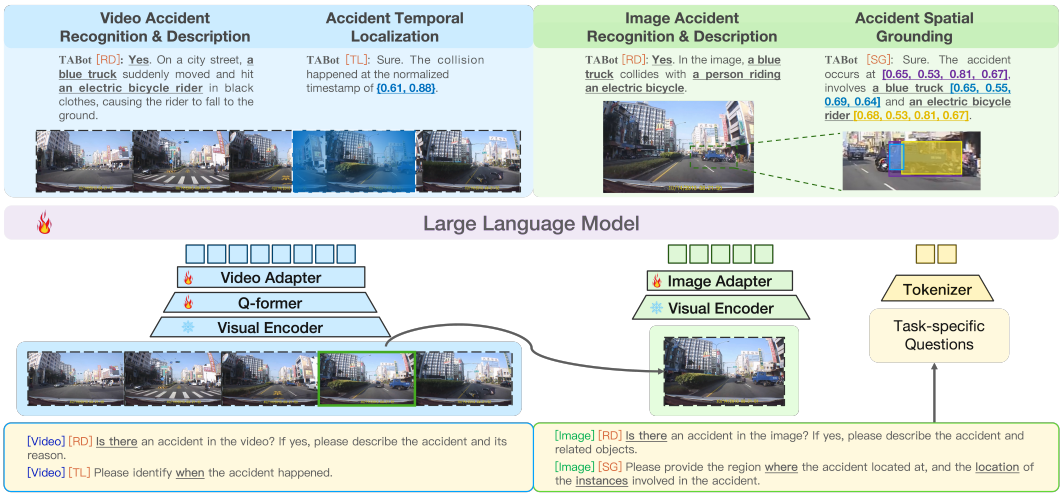


Figure 4: The model architecture and functional capabilities of the TABot.

scriptions are detailed and diverse, covering a broad range of traffic scenarios, accident types, and objects involved, as shown in the word cloud of accident descriptions in Figure 3(c).

We provide a more comprehensive comparison between TAU-106K and other datasets, focusing on key features such as size, domain, annotation types, and the characteristics of the textual captions, depicted in Table 1. According to the comparison, our TAU-106K is the largest dataset in terms of the number of videos and the diversity of annotations, supporting a wide range of tasks. In particular, benefiting from our manual annotation process that is labor-intensive yet worthy, the labeled free-form accident captions in TAU-106K are much more diverse and detailed than other datasets, achieving a largest average length of 32.1 words per caption. This makes TAU-106K a valuable resource for training and evaluating accident-aware models in traffic video understanding.

## 4 TABot: A Chatbot for Traffic Accident Understanding

We introduce TABot, a multimodal fine-grained MLLM developed by leveraging instructional data constructed from the TAU-106K dataset. TABot is compatible with both video and image modalities, enabling it to perform fine-grained understanding and reasoning tasks in traffic accident scenarios. The proposed TABot integrates a suite of traffic accident-related tasks, as depicted in Figure 4.

### 4.1 Model Overview

We advance the TABot upon GroundingGPT (Li et al., 2024), a model known for its strong performance in fine-grained image and video understanding. By fine-tuning this general-purpose MLLM on our annotated TAU-106K dataset, we enhance its capabilities for traffic accident comprehension on several functional tasks including Accident Recognition, Accident Description Generation, Accident Temporal Localization, and Accident Spatial Grounding, as illustrated in Figure 4. It is notable that we normalize the responses to the temporal localization and spatial grounding tasks to the video duration and image size, respectively, to ensure consistency and facilitate model training. The normalized responses are denoted as $\{t_{start}, t_{end}\}$ for temporal localization and $[x_{min}, y_{min}, x_{max}, y_{max}]$ for spatial grounding, enclosed in specific tokens to indicate the temporal boundaries and spatial regions.

Following previous works (Li et al., 2024), we adopt a two-stage fine-tuning approach: Firstly, during the functional tuning stage, TABot is jointly fine-tuned on both image and video data, focusing on the four key tasks mentioned above. We generate structured single-round conversations for each task to facilitate the model's understanding of traffic accidents from different perspectives. Two additional training strategies are proposed to further improve performance in temporal localization: Negative Segment Referring (NSR) and Video Spatial Alignment (VSA), which promote the performance from the perspective of contrastive learning and spatial understanding, respectively. NSR samples accident-free segments before the occurrence of an accident and trains the model by referring to the sample segments containing no accidents, serving as negative data to highlight the

perception of accident occurrences. On the other hand, benefiting from the unified video-to-image annotation pipeline, VSA involves the spatial grounding annotations into the video training process, complementing spatial information from images into the temporal localization task. As for the implementation details, we extend the answer to the temporal localization task to include the spatial grounding annotations. For example, the response to the temporal localization task '{*0.30, 0.45*}' may be further extended with "*At the timestamp 0.38, an accident occurs at the region of [0.21, 0.35, 0.87, 0.57].*" This alignment improves TABot's fine-grained spatial understanding of accidents in video contexts. Additionally, to ensure the model's flexibility in handling multiple tasks, task-specific flag tokens (Accident Recognition & Description [RD], Temporal Localization [TL], and Spatial Grounding [SG]) are inserted at the start of each query to guide TABot's responses.

With the above functional tuning, TABot is endowed with the capabilities to perform coarse- and fine-grained traffic accident understanding tasks. To further advance the TABot's comprehensive understanding and conversational skills, we utilize the textual captions of the video clips and images as the abstracts to prompt the powerful LLMs (Achiam et al., 2023), to conclude the above functional tasks and generate additional accident-oriented dialogue, such as the causes of accidents or prevention suggestions. The generated multi-round dialogue set is then used to instruct the TABot model. Through such instruction tuning, TABot is upgraded to a chat version (TABot-Chat) with enhanced instruction-following capabilities and a more comprehensive understanding of traffic accidents. In particular, the task flag tokens are maintained in the instruction tuning stage to guide the model's responses to specific tasks, ensuring the functional capabilities of the model towards multiple accident-oriented tasks.

## 5 EXPERIMENTS

We set GroundingGPT-7B (Li et al., 2024), a pre-trained general-purpose MLLM with temporal and spatial grounding capabilities, as the baseline model for our TABot. The detailed experimental settings of the two-step approach are described as follows:

**Functional Tuning.** We train LLM and both visual adapters of the GroundingGPT model through our TAU-106K dataset for 3 epochs using 8 $\times$ H800 GPUs. The initial learning rate is set to 2e-5 with a batch size of 32, requiring about 20 hours to complete.

**Instruction Tuning.** We extend training with the instruction-tuning dataset generated by LLaMA-70B (Dubey et al., 2024), leading to our TABot-Chat model. To avoid catastrophic forgetting, we combine the single-round and multi-round dialogue conversations during this stage, further training the model for 1 epoch on 8 $\times$ H800 GPUs for about 9 hours with the learning rate and batch size unchanged.

**Evaluation Metrics.** For evaluation purposes, the TAU-106K dataset was split into training and testing sets in a 9:1 ratio, ensuring the same distribution of normal/accident instances and scene continuity across both. We evaluate the TABot on four functional tasks for both image and video data. The evaluation metrics are as follows:

*1) Accident Recognition.* Recall, Precision, and F1 scores are used to assess the model's accuracy in distinguishing accidents from normal scenes in both image-level and video-level contexts.

*2) Accident Description.* BLEU-1 score, Rouge-L F1 score, and BERT F1 score are employed to measure the model's ability to generate coherent and accurate accident descriptions. We further leverage GPT-4o to estimate the quality of the generated descriptions, referred to as GPT-4 score.

*3) Accident Temporal Localization.* We reported the Intersection over Union (IoU) between predicted and true temporal intervals, along with Average Precision (AP@30, AP@50, AP@70).

*4) Accident Spatial Grounding.* We evaluate the model's performance on accident region and object grounding through reporting detection metrics: mean Intersection over Union (mIoU) and Average Precision (AP@30, AP@50, AP@70).

### 5.1 VIDEO-LEVEL TASKS

In this subsection, we present the results on video-level tasks of our proposed models, including TABot, TABot-Chat, and their comparison with several existing methods: Video-LLaVA (Lin et al.,

2023), TimeChat (Ren et al., 2024), VTimeLLM (Huang et al., 2024), GroundingGPT (Li et al., 2024), Qwen2-VL (Wang et al., 2024), and Gemini-1.5-Pro (Reid et al., 2024).

Table 2: Experimental results on video accident recognition in traffic scenes. "@A" and "@N" represent the class-wise results on accidents and normal scenes.

| Methods | Video Accident Recognition | | | | | | |
|---|---|---|---|---|---|---|---|
| | Acc | Rec@A | Pre@A | F@A | Rec@N | Pre@N | F1@N |
| Video-LLaVA (Lin et al., 2023) | 50.20 | 99.70 | 50.10 | 66.69 | 0.70 | 70.00 | 1.39 |
| TimeChat (Ren et al., 2024) | 54.65 | 91.80 | 52.67 | 66.93 | 17.50 | 68.09 | 27.84 |
| VTimeLLM (Huang et al., 2024) | 50.00 | **100.00** | 50.00 | 66.67 | 0.00 | 0.00 | 0.00 |
| GroundingGPT (Li et al., 2024) | 50.00 | **100.00** | 50.00 | 66.67 | 0.00 | 0.00 | 0.00 |
| Qwen2-VL (Wang et al., 2024) | 72.65 | 53.46 | 87.23 | 66.29 | 92.08 | 66.16 | 77.00 |
| Gemini-1.5-Pro (Reid et al., 2024) | 69.61 | 61.82 | 74.18 | 67.44 | 77.70 | 66.25 | 71.52 |
| **TABot (Ours)** | 81.00 | 78.65 | 85.10 | 81.75 | 83.77 | 76.90 | 80.19 |
| **TABot-Chat (Ours)** | **82.05** | 79.70 | 86.00 | **82.73** | 84.80 | **78.10** | **81.31** |

As presented in Table 2, most previous models struggle to recognize traffic accidents, with accuracies ranging from 50% to 54.65%. VTimeLLM and our baseline Grounding tend to classify all videos as abnormal, indicating several false positives. Although Qwen2-VL and Gemini-1.5-Pro show some improvement, they tend to classify the videos as normal, exhibiting a lack of accident perception. In contrast, our TABot, trained on our TAU-106K dataset, demonstrates a significant improvement, reaching an accuracy of 80.95% and outperforming all prior methods. Further instruction tuning with multi-round dialogue data, our TABot-Chat variant further presents an accuracy of 82.05% and improved overall performance for both accident and normal scenarios.

Table 3: Experimental results on video accident description and accident temporal localization.

| Methods | Video Accident Description | | | | Accident Temporal Localization | | | |
|---|---|---|---|---|---|---|---|---|
| | BLEU | Rouge | BERT | GPT-4 | AP@30 | AP@50 | AP@70 | mIoU |
| Video-LLaVA (Lin et al., 2023) | 22.20 | 24.81 | 60.72 | 26.17 | - | - | - | - |
| TimeChat (Ren et al., 2024) | 7.12 | 18.16 | 58.77 | 12.67 | 23.00 | 7.90 | 2.50 | 18.07 |
| VTimeLLM (Huang et al., 2024) | 25.25 | 23.32 | 60.84 | 18.62 | - | - | - | - |
| GroundingGPT (Li et al., 2024) | 9.77 | 16.43 | 55.70 | 14.00 | 4.60 | 2.40 | 0.90 | 3.79 |
| Qwen2-VL (Wang et al., 2024) | 15.38 | 23.64 | 61.61 | 39.80 | 32.91 | 15.76 | 5.42 | 20.75 |
| Gemini-1.5-Pro (Reid et al., 2024) | 12.83 | 19.57 | 60.79 | 23.66 | 13.87 | 5.14 | 1.64 | 9.31 |
| **TABot (Ours)** | 54.59 | 57.94 | 82.31 | 55.60 | **39.44** | 20.12 | **9.80** | **25.93** |
| **TABot-Chat (Ours)** | **55.70** | **58.32** | **83.78** | **55.73** | 37.90 | **20.70** | 7.80 | 25.33 |

For the tasks of video accident description and temporal localization, the performance of our models is detailed in Table 3. TABot excels in generating accurate and contextually relevant accident descriptions, achieving the highest BERT and GPT-4 scores, indicating high semantic alignment with human judgments. As for the most challenging task of accident temporal localization, previous models struggled to pinpoint the occurrence of accidents, and only Qwen2-VL demonstrated a certain capability in fine-grained localization within videos. Our TABot also significantly surpasses all existing methods in this fine-grained task, establishing a new state-of-the-art in temporal localization performance. After instruction tuning, the TABot-Chat variant shows improved description capabilities as we expected, with a slight decrease in temporal localization performance. This decrease can be attributed to the model's enhanced conversational abilities, which may lead to a slight decline in the model's focus on temporal localization.

### 5.2 Image-level Tasks

In addition to the video-level tasks, we also evaluate our proposed models on image-level tasks. The experimental results are presented in Tables 4 and 5, where we compare our models against several state-of-the-art methods (Zhu et al., 2023; Li et al., 2024; Bai et al., 2023; Wang et al., 2024; Reid et al., 2024; Achiam et al., 2023).

Table 4 presents the results of the image accident recognition. Our TABot outperforms all methods in image accident recognition, demonstrating the quality of our dataset and the effectiveness of our training strategies. As for accident description, the superior performance of our models is evident, validating that our model excels in generating accurate and contextually relevant descriptions of accidents. TABot-Chat, following instruction tuning, attains excellent values of 77.26 and 55.73 for BERT and GPT-4 scores, indicating high semantic alignment with human judgments.

Table 4: Experimental results on image accident recognition and description in traffic scenes.

| Methods | Image Accident Recognition | | | | | | | Image Accident Description | | | |
|---|---|---|---|---|---|---|---|---|---|---|---|
| | Acc | Rec@A | Pre@A | F1@A | Rec@N | Pre@N | F1@N | BLEU | Rouge | BERT | GPT-4 |
| MiniGPT4 (Zhu et al., 2023) | 64.05 | 75.57 | 68.89 | 72.08 | 45.73 | 54.06 | 49.54 | 9.63 | 11.56 | 45.84 | 11.67 |
| GroundingGPT (Li et al., 2024) | 63.75 | 79.15 | 67.45 | 72.84 | 39.25 | 54.20 | 45.53 | 7.22 | 7.81 | 45.00 | 21.08 |
| Qwen-VL-Max (Bai et al., 2023) | 69.95 | 87.87 | 70.48 | 78.22 | 41.45 | 68.23 | 51.57 | 4.59 | 4.27 | 43.08 | 28.46 |
| Qwen2-VL (Wang et al., 2024) | 58.35 | 40.07 | 83.53 | 54.16 | 87.44 | 47.84 | 61.84 | 23.31 | 24.53 | 66.12 | 32.01 |
| Gemini-1.5-Pro (Reid et al., 2024) | 80.99 | 0.00 | 0.00 | 0.00 | 80.99 | 1.00 | 89.50 | 16.28 | 21.53 | 64.44 | 24.54 |
| GPT-4o (Achiam et al., 2023) | 63.65 | 45.44 | 90.73 | 60.55 | **92.62** | 51.62 | 66.30 | 4.78 | 5.18 | 43.05 | 35.71 |
| **TABot (Ours)** | **90.75** | 94.38 | **90.31** | **92.30** | 85.58 | 91.45 | **88.42** | 48.62 | 43.31 | 75.20 | 55.12 |
| **TABot-Chat (Ours)** | 90.50 | **94.90** | 89.33 | 92.03 | 84.48 | **92.36** | 88.24 | **50.28** | **45.67** | **77.26** | **55.73** |

Table 5: Experimental results on accident region and object grounding in traffic images.

| Methods | Accident Region Grounding | | | | Accident Object Grounding | | | |
|---|---|---|---|---|---|---|---|---|
| | AP@30 | AP@50 | AP@70 | mIoU | AP@30 | AP@50 | AP@70 | mIoU |
| MiniGPT4 (Zhu et al., 2023) | 50.57 | 34.85 | 24.67 | 39.36 | 70.33 | 56.65 | 33.24 | 49.72 |
| GroundingGPT (Li et al., 2024) | 26.55 | 14.25 | 7.82 | 3.84 | 62.23 | 49.06 | 27.34 | 43.75 |
| Qwen-VL-Max (Bai et al., 2023) | 43.73 | 26.47 | 12.79 | 30.72 | 59.97 | 45.27 | 28.25 | 43.00 |
| Qwen2-VL (Wang et al., 2024) | 60.21 | 47.52 | 29.70 | 43.02 | 71.66 | 57.48 | 35.66 | 50.38 |
| Gemini-1.5-Pro (Reid et al., 2024) | 56.66 | 37.20 | 17.42 | 37.85 | 46.07 | 34.99 | 20.09 | 31.98 |
| **TABot (Ours)** | 80.05 | **70.03** | **45.52** | **57.83** | **78.05** | **65.86** | **39.88** | **54.95** |
| **TABot-Chat (Ours)** | **80.29** | 69.87 | 44.95 | 57.63 | 77.64 | 65.41 | 39.68 | 54.78 |

Table 5 showcases the results for region- and object-level grounding. Our TABot significantly outperforms the baselines in terms of AP and mIoU for both accident regions and objects. Similar to the phenomenon observed in video tasks, instruction tuning slightly perturbs the model's grounding performance, but the overall performance remains competitive. The essential fine-grained grounding performance gap compared to previous methods further highlights the necessity of collecting traffic accident data and training models on this specific domain.

### 5.3 Ablation Study

**The Effectiveness of Joint Training.** To evaluate the impact of joint training on image and video data, we additionally train the TABot using a single modality (TABot-single trained on image or video data only) and compare the results with our joint training model (TABot). According to the main results in Tables 6, the joint training model outperforms the single modality models in most tasks, especially for image-level tasks. The improvement in accident recognition and description tasks is more pronounced than in spatial grounding tasks, indicating that the primary benefit of video data is the scale-up in the amount of training data, which is particularly effective for tasks requiring richer contextual information. On the other hand, incorporating image data into video tasks leads to a minor performance drop, suggesting that the model's focus on video data may have slightly compromised its performance on image tasks.

**The Effectiveness of VSA and NSR.** Benefiting from our unified video-image annotation pipeline, VSA can explicitly incorporate spatial grounding annotations at specific time frames into the training of video temporal localization. As shown in Table 7, our VSA strategy leads to a consistent improvement in the model's temporal localization capabilities, demonstrating its effectiveness in involving spatial information as a complementary signal to enhance the model's temporal perception. As for NSR, it improves the model's overall performance across both image and video tasks by enhancing its capacity to differentiate accident events from normal content, as indicated in Table 7. However, there is a marginal decline in spatial grounding performance, and we attribute this to the model's focus on temporal localization, which may have led to a slight trade-off in spatial understanding. This drawback is compensated when the NSR is combined with the VSA, as all tasks achieve their best performance, demonstrating the complementary nature of these two strategies.

Table 6: Ablation study of separate (TABot-single) or joint (TABot) training on image and video data. "AG", "OG" & "TL" denote the AP@50 of Accident region Grounding, accident Object Grounding, and Temporal Localization.

| Model | Image Understanding | | | | | Video Understanding | | | |
|---|---|---|---|---|---|---|---|---|---|
| | Acc | BERT | GPT-4 | AG | OG | Acc | BERT | GPT-4 | TL |
| TABot-single | 77.95 | 74.16 | 48.22 | 68.97 | 64.70 | 80.95 | **82.62** | 54.63 | **20.28** |
| TABot | **90.75** | **75.20** | **55.12** | **70.03** | **65.86** | **81.00** | 82.31 | **55.60** | 20.12 |

Table 7: Ablation study on the additional training strategies.

| TABot | | Image Understanding | | | | | Video Understanding | | | |
|---|---|---|---|---|---|---|---|---|---|---|
| VSA | NSR | Acc | BERT | GPT-4 | AG | OG | Acc | BERT | GPT-4 | TL |
| ✗ | ✗ | 88.45 | 75.09 | 54.28 | 68.57 | 64.06 | 80.50 | 82.08 | 55.23 | 19.30 |
| ✗ | ✓ | 88.00 | 74.73 | 53.82 | 70.20 | 64.21 | **81.90** | 81.72 | 54.78 | 18.90 |
| ✓ | ✗ | 88.60 | 74.83 | 53.91 | **70.36** | 64.55 | 80.80 | 82.26 | 55.53 | 19.92 |
| ✓ | ✓ | **90.75** | **75.20** | **55.12** | 70.03 | **65.86** | 81.00 | **82.31** | **55.60** | **20.12** |

Table 8: Ablation study on the training strategy of the **instructing tuning**.

| TABot-Chat | | Image Understanding | | | | | Video Understanding | | | |
|---|---|---|---|---|---|---|---|---|---|---|
| Mixed Data | Task Flag | Acc | BERT | GPT-4 | AG | OG | Acc | BERT | GPT-4 | TL |
| ✗ | ✗ | 84.55 | 75.44 | 50.18 | 68.71 | 64.52 | 79.50 | 82.43 | 53.32 | 5.10 |
| ✗ | ✓ | 85.50 | 75.59 | 52.83 | 69.14 | 64.76 | 79.35 | 82.14 | 54.51 | 13.30 |
| ✓ | ✗ | 88.30 | 76.56 | 52.04 | 69.22 | 64.11 | 80.20 | 83.10 | 55.40 | 18.90 |
| ✓ | ✓ | **90.45** | **77.20** | **55.73** | **69.46** | **64.96** | **81.25** | **83.51** | **55.73** | **19.50** |

**Training Strategies for Chat Version** In the TABot-Chat model, we observe that directly performing instruction tuning without additional recipes significantly degrades the model's performance in functional tasks, for example, the accuracy for image accident recognition decreased to 84.55%. To maintain or even improve the functional performance, we took some data-centric approaches: (1) mix the datasets used for Functional Tuning and Instruction Tuning. (2) introduce task flags to specify the target response for the model in a multi-task framework. As presented in Table 8, based on our training data paradigm, we successfully improve the conversational performance of TABot-Chat while maintaining excellent functional results.

Table 9: The ablation study of reasoning captions on the temporal localization task.

| Model | AP@30 | AP@50 | AP@70 | mIoU |
|---|---|---|---|---|
| TABot | 39.44 | 20.12 | 9.80 | 25.93 |
| - Reason Caption | 34.20 | 16.90 | 6.60 | 21.67 |

**Effectiveness of Reasoning Description** In the application of MLLMs to traffic accident understanding, the most critical task is to achieve precise temporal localization of accidents in videos. The labeled reason caption in our TAU-106K dataset is a portent of the content of the accident, which makes accident detection and localization more trackable. Here we evaluate the effectiveness of the reasoning caption in the temporal localization task by conducting an ablation study as shown in Table 9. The results show that the removal of reasoning captions leads to a significant performance drop in the temporal localization task, validating our claim that reasoning captions serve as valuable cues for accident understanding. Our future work will focus on developing more reasoning tasks based on the reasoning captions in TAU-106K to achieve accident forecasting and causality analysis tasks.

## 6 Discussion and Conclusion

To advance the exploration of multimodal language learning models (MLLM) for traffic accident understanding, we introduced video-image-text joint dataset TAU-106K, which includes 51.5K video clips and 54.8K images, with high-quality annotations covering coarse- and fine-grained accident-oriented information. Upon our comprehensive dataset, we proposed TABot, a unified MLLM that is compatible with video and image data and can handle various traffic accident understanding tasks including accident recognition, description, temporal localization, and spatial grounding. Our method and dataset lay the foundation for MLLM to infer and understand fine-grained representations of traffic accident scenarios. Our publicly available data and code will facilitate further research on MLLM for traffic accidents. Future work will include more detailed grounding and addressing the hallucination problem.

### Acknowledgments

This work was partially supported by the National Natural Science Foundation of China under Grants No. 62222203 and the New Cornerstone Science Foundation through the XPLORER PRIZE.

## REFERENCES

Josh Achiam, Steven Adler, Sandhini Agarwal, Lama Ahmad, Ilge Akkaya, Florencia Leoni Aleman, Diogo Almeida, Janko Altenschmidt, Sam Altman, Shyamal Anadkat, et al. Gpt-4 technical report. *arXiv preprint arXiv:2303.08774*, 2023.

Lisa Anne Hendricks, Oliver Wang, Eli Shechtman, Josef Sivic, Trevor Darrell, and Bryan Russell. Localizing moments in video with natural language. In *Proceedings of the IEEE international conference on computer vision*, pp. 5803–5812, 2017.

Jinze Bai, Shuai Bai, Shusheng Yang, Shijie Wang, Sinan Tan, Peng Wang, Junyang Lin, Chang Zhou, and Jingren Zhou. Qwen-vl: A frontier large vision-language model with versatile abilities. *arXiv preprint arXiv:2308.12966*, 2023.

Wentao Bao, Qi Yu, and Yu Kong. Uncertainty-based traffic accident anticipation with spatio-temporal relational learning. In *Proceedings of the 28th ACM International Conference on Multimedia*, pp. 2682–2690, 2020.

Yunkang Cao, Xiaohao Xu, Chen Sun, Xiaonan Huang, and Weiming Shen. Towards generic anomaly detection and understanding: Large-scale visual-linguistic model (gpt-4v) takes the lead. *arXiv preprint arXiv:2311.02782*, 2023.

Fu-Hsiang Chan, Yu-Ting Chen, Yu Xiang, and Min Sun. Anticipating accidents in dashcam videos. In *Computer Vision–ACCV 2016: 13th Asian Conference on Computer Vision, Taipei, Taiwan, November 20-24, 2016, Revised Selected Papers, Part IV 13*, pp. 136–153. Springer, 2017.

Guo Chen, Yin-Dong Zheng, Jiahao Wang, Jilan Xu, Yifei Huang, Junting Pan, Yi Wang, Yali Wang, Yu Qiao, Tong Lu, et al. Videollm: Modeling video sequence with large language models. *arXiv preprint arXiv:2305.13292*, 2023a.

Jun Chen, Deyao Zhu, Xiaoqian Shen, Xiang Li, Zechun Liu, Pengchuan Zhang, Raghuraman Krishnamoorthi, Vikas Chandra, Yunyang Xiong, and Mohamed Elhoseiny. Minigpt-v2: large language model as a unified interface for vision-language multi-task learning. *arXiv preprint arXiv:2310.09478*, 2023b.

Keqin Chen, Zhao Zhang, Weili Zeng, Richong Zhang, Feng Zhu, and Rui Zhao. Shikra: Unleashing multimodal llm's referential dialogue magic. *arXiv preprint arXiv:2306.15195*, 2023c.

Zhe Chen, Jiannan Wu, Wenhai Wang, Weijie Su, Guo Chen, Sen Xing, Muyan Zhong, Qinglong Zhang, Xizhou Zhu, Lewei Lu, Bin Li, Ping Luo, Tong Lu, Yu Qiao, and Jifeng Dai. Internvl: Scaling up vision foundation models and aligning for generic visual-linguistic tasks. *arXiv preprint arXiv:2312.14238*, 2023d.

Zhe Chen, Weiyun Wang, Hao Tian, Shenglong Ye, Zhangwei Gao, Erfei Cui, Wenwen Tong, Kongzhi Hu, Jiapeng Luo, Zheng Ma, et al. How far are we to gpt-4v? closing the gap to commercial multimodal models with open-source suites. *arXiv preprint arXiv:2404.16821*, 2024.

Zesen Cheng, Sicong Leng, Hang Zhang, Yifei Xin, Xin Li, Guanzheng Chen, Yongxin Zhu, Wenqi Zhang, Ziyang Luo, Deli Zhao, et al. Videollama 2: Advancing spatial-temporal modeling and audio understanding in video-llms. *arXiv preprint arXiv:2406.07476*, 2024.

Abhimanyu Dubey, Abhinav Jauhri, Abhinav Pandey, Abhishek Kadian, Ahmad Al-Dahle, Aiesha Letman, Akhil Mathur, Alan Schelten, Amy Yang, Angela Fan, et al. The llama 3 herd of models. *arXiv preprint arXiv:2407.21783*, 2024.

Jianwu Fang, Dingxin Yan, Jiahuan Qiao, Jianru Xue, and Hongkai Yu. Dada: Driver attention prediction in driving accident scenarios. *IEEE transactions on intelligent transportation systems*, 23(6):4959–4971, 2021.

Jianwu Fang, Lei-Lei Li, Kuan Yang, Zhedong Zheng, Jianru Xue, and Tat-Seng Chua. Cognitive accident prediction in driving scenes: A multimodality benchmark. *arXiv preprint arXiv:2212.09381*, 2022a.

Jianwu Fang, Jiahuan Qiao, Jie Bai, Hongkai Yu, and Jianru Xue. Traffic accident detection via self-supervised consistency learning in driving scenarios. *IEEE Transactions on Intelligent Transportation Systems*, 23(7):9601–9614, 2022b.

Jiyang Gao, Chen Sun, Zhenheng Yang, and Ram Nevatia. Tall: Temporal activity localization via language query. In *Proceedings of the IEEE international conference on computer vision*, pp. 5267–5275, 2017.

Hadi Ghahremannezhad, Hang Shi, and Chengjun Liu. Real-time accident detection in traffic surveillance using deep learning. In *2022 IEEE international conference on imaging systems and techniques (IST)*, pp. 1–6. IEEE, 2022.

Sanjay Haresh, Sateesh Kumar, M Zeeshan Zia, and Quoc-Huy Tran. Towards anomaly detection in dashcam videos. In *2020 IEEE Intelligent Vehicles Symposium (IV)*, pp. 1407–1414. IEEE, 2020.

Mahmudul Hasan, Jonghyun Choi, Jan Neumann, Amit K Roy-Chowdhury, and Larry S Davis. Learning temporal regularity in video sequences. In *Proceedings of the IEEE conference on computer vision and pattern recognition*, pp. 733–742, 2016.

Bo He, Hengduo Li, Young Kyun Jang, Menglin Jia, Xuefei Cao, Ashish Shah, Abhinav Shrivastava, and Ser-Nam Lim. Ma-lmm: Memory-augmented large multimodal model for long-term video understanding. In *Proceedings of the IEEE/CVF Conference on Computer Vision and Pattern Recognition*, pp. 13504–13514, 2024.

Bin Huang, Xin Wang, Hong Chen, Zihan Song, and Wenwu Zhu. Vtimellm: Empower llm to grasp video moments. In *Proceedings of the IEEE/CVF Conference on Computer Vision and Pattern Recognition*, pp. 14271–14280, 2024.

Caitlienne Diane C Juan, Jaira Rose A Bat-og, Kimberly K Wan, and Macario O Cordel II. Investigating visual attention-based traffic accident detection model. *Philippine Journal of Science*, 150 (2), 2021.

Hoon Kim, Kangwook Lee, Gyeongjo Hwang, and Changho Suh. Crash to not crash: Learn to identify dangerous vehicles using a simulator. In *Proceedings of the AAAI Conference on Artificial Intelligence*, volume 33, pp. 978–985, 2019.

Ranjay Krishna, Kenji Hata, Frederic Ren, Li Fei-Fei, and Juan Carlos Niebles. Dense-captioning events in videos. In *Proceedings of the IEEE international conference on computer vision*, pp. 706–715, 2017.

Junnan Li, Dongxu Li, Silvio Savarese, and Steven Hoi. Blip-2: Bootstrapping language-image pre-training with frozen image encoders and large language models. In *International conference on machine learning*, pp. 19730–19742. PMLR, 2023.

Zhaowei Li, Qi Xu, Dong Zhang, Hang Song, Yiqing Cai, Qi Qi, Ran Zhou, Junting Pan, Zefeng Li, Van Tu Vu, et al. Groundinggpt: Language enhanced multi-modal grounding model. *arXiv preprint arXiv:2401.06071*, 2024.

Rongqin Liang, Yuanman Li, Jiantao Zhou, and Xia Li. Text-driven traffic anomaly detection with temporal high-frequency modeling in driving videos. *IEEE Transactions on Circuits and Systems for Video Technology*, 2024.

Bin Lin, Bin Zhu, Yang Ye, Munan Ning, Peng Jin, and Li Yuan. Video-llava: Learning united visual representation by alignment before projection. *arXiv preprint arXiv:2311.10122*, 2023.

Haotian Liu, Chunyuan Li, Qingyang Wu, and Yong Jae Lee. Visual instruction tuning. *Advances in neural information processing systems*, 36, 2024.

Hui Lv, Chuanwei Zhou, Zhen Cui, Chunyan Xu, Yong Li, and Jian Yang. Localizing anomalies from weakly-labeled videos. *IEEE transactions on image processing*, 30:4505–4515, 2021.

Muhammad Maaz, Hanoona Rasheed, Salman Khan, and Fahad Shahbaz Khan. Video-chatgpt: Towards detailed video understanding via large vision and language models. *arXiv preprint arXiv:2306.05424*, 2023.

Zhiliang Peng, Wenhui Wang, Li Dong, Yaru Hao, Shaohan Huang, Shuming Ma, and Furu Wei. Kosmos-2: Grounding multimodal large language models to the world. *arXiv preprint arXiv:2306.14824*, 2023.

Long Qian, Juncheng Li, Yu Wu, Yaobo Ye, Hao Fei, Tat-Seng Chua, Yueting Zhuang, and Siliang Tang. Momentor: Advancing video large language model with fine-grained temporal reasoning. *arXiv preprint arXiv:2402.11435*, 2024.

Machel Reid, Nikolay Savinov, Denis Teplyashin, Dmitry Lepikhin, Timothy Lillicrap, Jean-baptiste Alayrac, Radu Soricut, Angeliki Lazaridou, Orhan Firat, Julian Schrittwieser, et al. Gemini 1.5: Unlocking multimodal understanding across millions of tokens of context. *arXiv preprint arXiv:2403.05530*, 2024.

Shuhuai Ren, Linli Yao, Shicheng Li, Xu Sun, and Lu Hou. Timechat: A time-sensitive multimodal large language model for long video understanding. In *Proceedings of the IEEE/CVF Conference on Computer Vision and Pattern Recognition*, pp. 14313–14323, 2024.

Ankit Parag Shah, Jean-Bapstite Lamare, Tuan Nguyen-Anh, and Alexander Hauptmann. Cadp: A novel dataset for cctv traffic camera based accident analysis. In *2018 15th IEEE International Conference on Advanced Video and Signal Based Surveillance (AVSS)*, pp. 1–9. IEEE, 2018.

Gemini Team, Petko Georgiev, Ving Ian Lei, Ryan Burnell, Libin Bai, Anmol Gulati, Garrett Tanzer, Damien Vincent, Zhufeng Pan, Shibo Wang, et al. Gemini 1.5: Unlocking multimodal understanding across millions of tokens of context. *arXiv preprint arXiv:2403.05530*, 2024.

Peng Wang, Shuai Bai, Sinan Tan, Shijie Wang, Zhihao Fan, Jinze Bai, Keqin Chen, Xuejing Liu, Jialin Wang, Wenbin Ge, et al. Qwen2-vl: Enhancing vision-language model's perception of the world at any resolution. *arXiv preprint arXiv:2409.12191*, 2024.

Li Xu, He Huang, and Jun Liu. Sutd-trafficqa: A question answering benchmark and an efficient network for video reasoning over traffic events. In *Proceedings of the IEEE/CVF conference on computer vision and pattern recognition*, pp. 9878–9888, 2021.

Mingze Xu, Mingfei Gao, Zhe Gan, Hong-You Chen, Zhengfeng Lai, Haiming Gang, Kai Kang, and Afshin Dehghan. Slowfast-llava: A strong training-free baseline for video large language models. *arXiv preprint arXiv:2407.15841*, 2024.

Yajun Xu, Chuwen Huang, Yibing Nan, and Shiguo Lian. Tad: A large-scale benchmark for traffic accidents detection from video surveillance. *arXiv preprint arXiv:2209.12386*, 2022.

An Yang, Baosong Yang, Binyuan Hui, Bo Zheng, Bowen Yu, Chang Zhou, Chengpeng Li, Chengyuan Li, Dayiheng Liu, Fei Huang, et al. Qwen2 technical report. *arXiv preprint arXiv:2407.10671*, 2024.

Yu Yao, Mingze Xu, Yuchen Wang, David J Crandall, and Ella M Atkins. Unsupervised traffic accident detection in first-person videos. In *2019 IEEE/RSJ International Conference on Intelligent Robots and Systems (IROS)*, pp. 273–280. IEEE, 2019.

Yu Yao, Xizi Wang, Mingze Xu, Zelin Pu, Yuchen Wang, Ella Atkins, and David J Crandall. Dota: Unsupervised detection of traffic anomaly in driving videos. *IEEE transactions on pattern analysis and machine intelligence*, 45(1):444–459, 2022.

Haoxuan You, Haotian Zhang, Zhe Gan, Xianzhi Du, Bowen Zhang, Zirui Wang, Liangliang Cao, Shih-Fu Chang, and Yinfei Yang. Ferret: Refer and ground anything anywhere at any granularity. *arXiv preprint arXiv:2310.07704*, 2023.

Hang Zhang, Xin Li, and Lidong Bing. Video-llama: An instruction-tuned audio-visual language model for video understanding. *arXiv preprint arXiv:2306.02858*, 2023.

Yuanhan Zhang, Bo Li, haotian Liu, Yong jae Lee, Liangke Gui, Di Fu, Jiashi Feng, Ziwei Liu, and Chunyuan Li. Llava-next: A strong zero-shot video understanding model, April 2024. URL `https://llava-vl.github.io/blog/2024-04-30-llava-next-video/`.

Deyao Zhu, Jun Chen, Xiaoqian Shen, Xiang Li, and Mohamed Elhoseiny. Minigpt-4: Enhancing vision-language understanding with advanced large language models. *arXiv preprint arXiv:2304.10592*, 2023.

Rixing Zhu, Jianwu Fang, Hongke Xu, and Jianru Xue. Progressive temporal-spatial-semantic analysis of driving anomaly detection and recounting. *Sensors*, 19(23):5098, 2019.